www.czasopisma.pan.pl PAN POLSKA AKADEMIA NAUK www.journals.pan.pl

Arch. Metall. Mater. **62** (2017), 2B, 1051-1056

DOI: 10.1515/amm-2017-0152

S.H. CHOI*,**, B. ALI*,***, K.S. CHOI****, S.K. HYUN**, J.J. SIM*,**, W.J. CHOI*, W. JOO*, J.H. LIM*, T.H. LEE*****, T.S. KIM*,***#, K.T. PARK*#

REACTION KINETICS AND MORPHOLOGICAL STUDY OF $TiNb_2O_7$ SYNTHESIZED BY SOLID-STATE REACTION

Although $TiNb_2O_7$ is regarded as a material with high application potential in lithium-ion batteries (LIBs) and solid-oxide fuel cells (SOFCs), it has been difficult to find suitable cost-effective conditions for synthesizing it on a commercial scale. In this study, $TiNb_2O_7$ compounds were synthesized by a solid state synthesis process. For stoichiometrically precise synthesis of the $TiNb_2O_7$ phase, the starting materials, TiO_2 and Nb_2O_5 were taken in a 1:1 molar ratio. Activation energy and reaction kinetics of the system were investigated at various synthesis temperatures (800,1000,1200, and 1400°C) and for various holding durations (1,5,10, and 20 h). Furthermore, change in the product morphology and particle size distribution were also evaluated as a function of synthesis temperature and duration. Additionally, quantitative phase analysis was conducted using the Rietveld refinement method. It was found that increases in the synthesis temperature and holding time lead to increase in the mean particle size from 1 to 4.5 µm. The reaction rate constant for the synthesis reaction was also calculated.

Keywords: $TiNb_2O_7$ synthesis, Solid state reaction, Kinetic analysis, Quantitative phase analysis

1. Introduction

$TiNb_2O_7$ ($TiO_2{\cdot}Nb_2O_5$) is regarded as one of the most promising alternative materials available for use in lithium ion batteries (LIBs) [1,2], solid oxide fuel cells (SOFCs) [3], electrochromic devices [4], and ceramic-based solid state humidity sensors [5]. $TiNb_2O_7$ can be synthesized by a variety of processes such as solid state synthesis [6], laser-induced pyrolysis [7], hydrothermal crystallization [8], and evaporation-induced self-assembly (EISA) [1].

In the large-scale production of SOFC or LIB energy storage devices, cost-effective and easy-to-handle methods for the fabrication of various components are required. From this point of view, solid state synthesis appears to be the most suitable method for producing large amounts of $TiNb_2O_7$. Jat et al. [6] have recently estimated the thermodynamic properties of Ti-Nb-O systems and synthesized $TiNb_2O_7$ by heat-treatment at 1000°C for 48 h in their studies. Reich et al [3]. have also studied $TiNb_2O_7$ as an anode material for SOFCs. In their study, $TiNb_2O_7$ was prepared by a standard solid state reaction at 1250°C for 48 h in air.

In the pseudo-binary TiO_2-Nb_2O_5 system (Fig. 1), three stable titanium niobates, namely $TiNb_2O_7$, $Ti_2Nb_{10}O_{29}$, and $TiNb_{24}O_{62}$ have been reported to occur [9]. Among these,

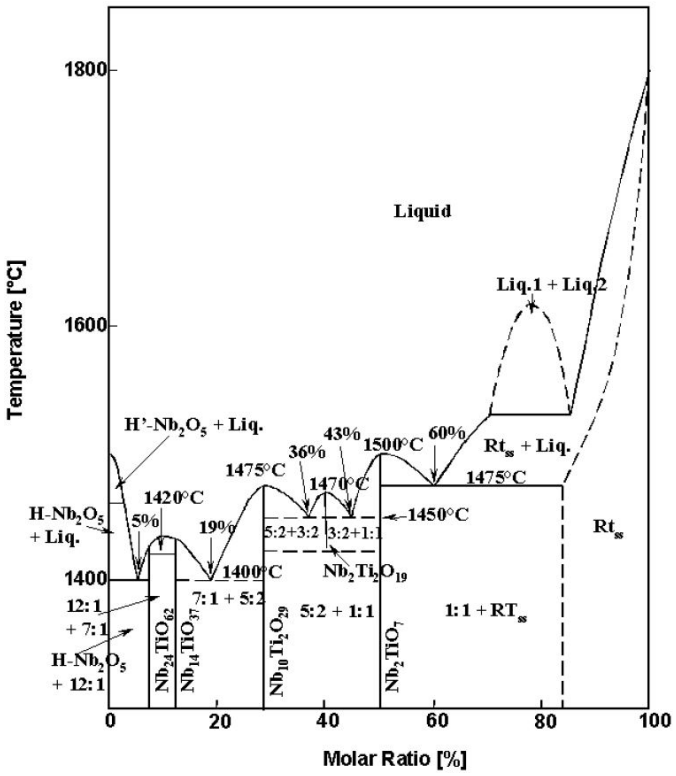

Fig. 1. Equilibrium diagram for the TiO_2-Nb_2O_5 system

* KOREA INSTITUTE FOR RARE METALS, KOREA INSTITUTE OF INDUSTRIAL TECHNOLOGY, ELEVENTH FLOOR, GET-PEARL TOWER, GAETBEOL-RO 12, YEONSU-GU, INCHEON, SOUTH KOREA
** DEPARTMENT OF ADVANCED MATERIALS ENGINEERING, IN-HA UNIVERSITY, INCHEON, SOUTH KOREA
*** DEPARTMENT OF CRITICAL MATERIALS AND SEMICONDUCTOR PACKAGING ENGINEERING, UNIVERSITY OF SCIENCE AND TECHNOLOGY, DAEJEON, SOUTH KOREA
**** DEPARTMENT OF MATERIALS SCIENCE AND ENGINEERING, SEOUL, SOUTH KOREA
***** DEPARTMENT OF MATERIALS SCIENCE & ENGINEERING, UNIVERSITY OF SHEFFIELD, SHEFFIELD S1 3JD, UNITED KINGDOM

Corresponding authors: ktpark@kitech.re.kr and tskim@kitech.re.kr

$TiNb_2O_7$ ($TiO_2{\cdot}Nb_2O_5$) and $Ti_2Nb_{10}O_{29}$ ($2TiO_2{\cdot}5Nb_2O_5$) were first reported by Roth and Coughanour [10,11], whereas Roth and Wedsley reported the existence of Nb_2O_5-rich $TiNb_{24}O_{62}$ ($TiO_2{\cdot}12Nb_2O_5$) [12].

As shown in TABLE 1 [9], these complexes differ in their physical properties and crystal structures. Out of the three oxides, $TiNb_2O_7$ has been considered to be the most suitable for use in LIBs and SOFCs. In particular, for using $TiNb_2O_7$ as an SOFC anode material, it is necessary to synthesize stoichiometrically exact $TiNb_2O_7$ with fine particles, in order to control the final morphology of the anode components. So far, studies on $TiNb_2O_7$ have focused on evaluating the performance of devices containing $TiNb_2O_7$ such as SOFCs and LIBs. Consequently, there is little information in the literature on the kinetics of synthesis as well as kinetic behavior of $TiNb_2O_7$.

TABLE 1

Characteristics of the TiO_2-Nb_2O_5 system as a function of phase composition

Composition (mole percent)		Temperature observed	
TiO_2	Nb_2O_5	Solidus	Liquidus
%	%	°C	°C
95	5	1,780	1,800
90	10	1,510	—
85.71	14.29	1,490	—
80	20	1,475	—
75	25	1,475	—
67	33	1,475	1,500
60	40	1,470	1,480
50	50	1,490	1,490
40	60	1,465	1,470
33	67	1,465	1,475
25	75	1,480	1,480
20	80	1,465	1,470
16.67	83.33	—	1,475
14.29	85.71	—	—
10	90	1,475	1,485
5	95	1,485	1,495
0	100	1,500	1,500

In the present study, $TiNb_2O_7$ was synthesized by a solid state reaction with a stoichiometric TiO_2/Nb_2O_5 molar ratio of 1:1. The phase composition of the synthesized product, fraction of $TiNb_2O_7$ in the product, and morphology were investigated as a function of synthesis temperature and dwell time.

2. Experimental

TiO_2 (Junsei Chemical Co., Ltd, 99%) and Nb_2O_5 (Junsei Chemical Co., Ltd, 99%) powders were used as the starting materials. For the precise synthesis of $TiNb_2O_7$, a stoichiometric molar ratio of TiO_2 and Nb_2O_5 (1:1) was mixed thoroughly in a mortar. The mixture was then placed in an alumina crucible and heated in an electric furnace at various temperatures (800,1000,1200, and 1400°C) and for various holding durations (1,10,15, and 20 h). A heating rate of 8°C/min was used for the synthesis. After heating, the samples were furnace-cooled to room temperature.

The starting materials and synthesized powders were characterized using various qualitative and quantitative techniques. The morphology of the powder particles was observed by field emission scanning electron microscopy (FE-SEM, Hitachi, SU-8010), while the phases in the materials were identified using X-ray diffraction (XRD, Bruker, D8 DISCOVER) using Cu Kα radiation (40 kV, 40 mA) with the 2θ values increased in step sizes of 0.004/0.5 s. The experimental temperature conditions were determined using differential thermal analysis (DTA, PerkinElmer, STA8000) up to 1400°C with a heating rate of 1°C /min. A particle size analyzer (PSA, Beckman Coulter LS I3 320, USA) was used to measure the size of the powder particles. For quantitative phase analysis (QPA), TOPAS (Bruker, Total Pattern Analysis Solution), a computer program based on the Rietveld refinement method was used. Using the QPA results, rate constants and activation energy (Eα) values were calculated using Arrhenius law.

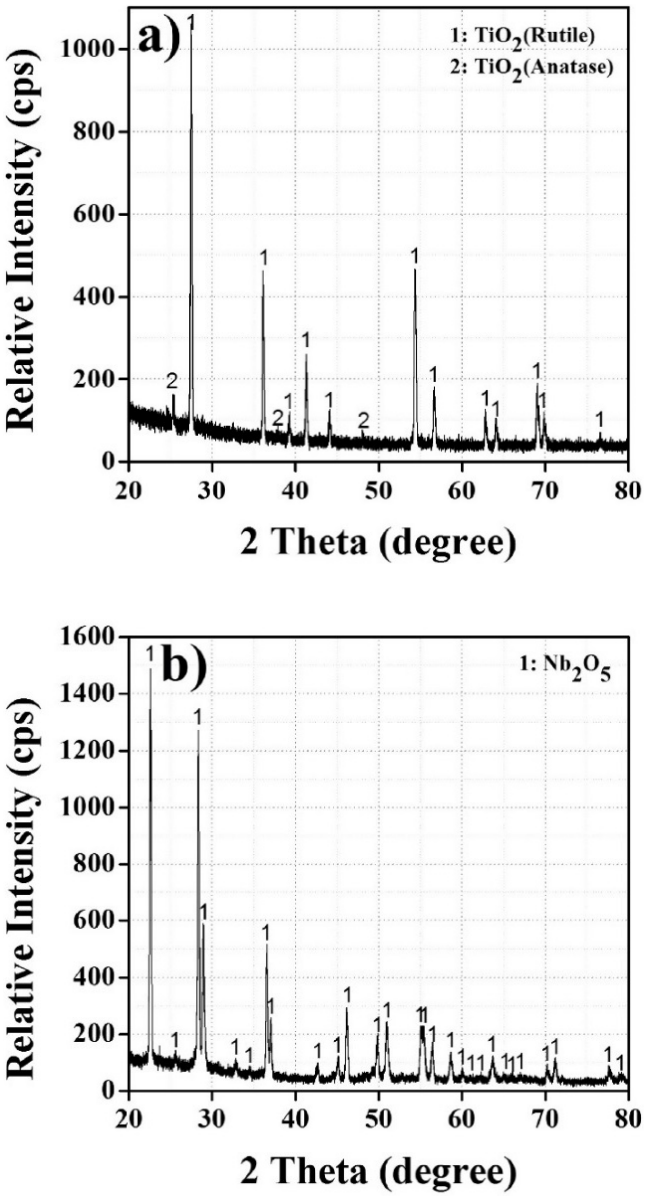

Fig. 2. X-ray diffraction patterns of the starting materials; a) TiO_2 powder and b) Nb_2O_5 powder

3. Results and discussion

3.1. Characterization of the TiO_2 and Nb_2O_5 powders

Results from the XRD analysis of the starting materials (TiO_2 and Nb_2O_5) are shown in Fig. 2. As evident from (Fig. 2a), the TiO_2 powder is mostly composed of the stable rutile phase along with a small amount of metastable anatase phase. On the other hand, the Nb_2O_5 powder does not contain any impurities (Fig. 2b). Further, from Fig. 3, which are SEM micrographs of TiO_2 and Nb_2O_5, it is evident that both the powders are agglomerated and exhibit irregular particle shapes.

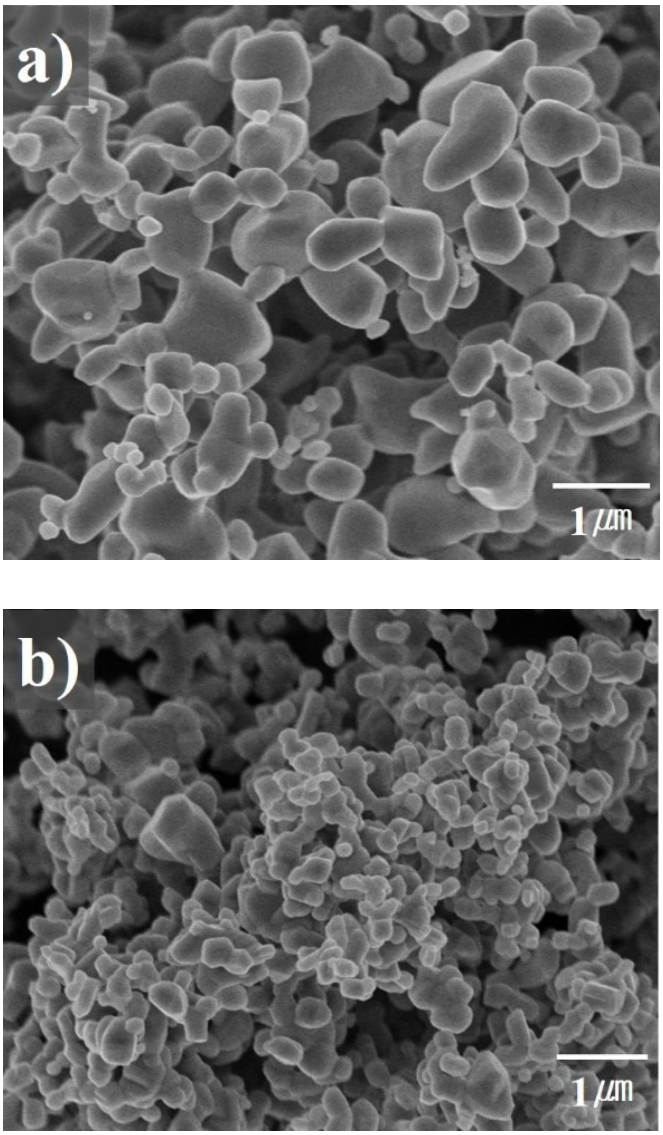

Fig. 3. SEM morphologies of the starting materials; a) TiO_2 powder and b) Nb_2O_5 powder

Fig. 4 shows the DTA curve of the TiO_2 and Nb_2O_5 powder mixture. This mixture was heated in an Ar atmosphere at a heating rate of 1°C/min up to a maximum temperature of 1400°C. An exothermic reaction was observed around 800°C, signaling the commencement of the synthesis reaction. Therefore, the synthesis temperatures were chosen in the range of 800 to 1400°C.

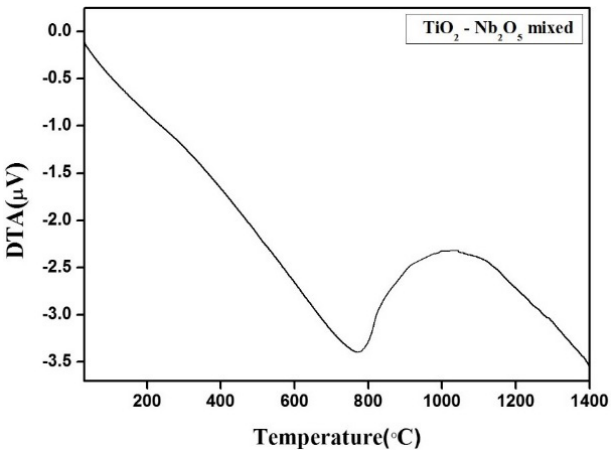

Fig. 4. DTA plot of the TiO_2-Nb_2O_5 mixed powder heated at a rate of 1°C /min

3.2. Synthesis mechanism of $TiNb_2O_7$

Fig. 5 shows the XRD patterns of the Ti-Nb-O powders synthesized by solid state reactions at (a) 800°C, (b) 1000°C, (c) 1200°C, and (d) 1400°C. It can be seen that at 800°C, upon increasing the processing time from 1 to 20 h (Fig. 5a), the Nb_2O_5 phase starts to disappear and the $TiNb_{24}O_{62}$ content starts to increase, forming a Nb_2O_5-rich TiO_2-Nb_2O_5 system. The Nb_2O_5 phase disappears completely after 20 h of processing, whereas the TiO_2 phase coexists with the $TiNb_{24}O_{62}$ and $Ti_2Nb_{10}O_{29}$ phases. At a synthesis temperature of 1000°C (Fig. 5b), Nb_2O_5 is not detected. At this temperature, the peak intensities corresponding to the TiO_2, $TiNb_{24}O_{62}$, and $Ti_2Nb_{10}O_{29}$ phases start to decrease, while the peak corresponding to the $TiNb_2O_7$ phase starts to increase in intensity with increase in the processing time. After 20 h of processing, $TiNb_2O_7$ becomes

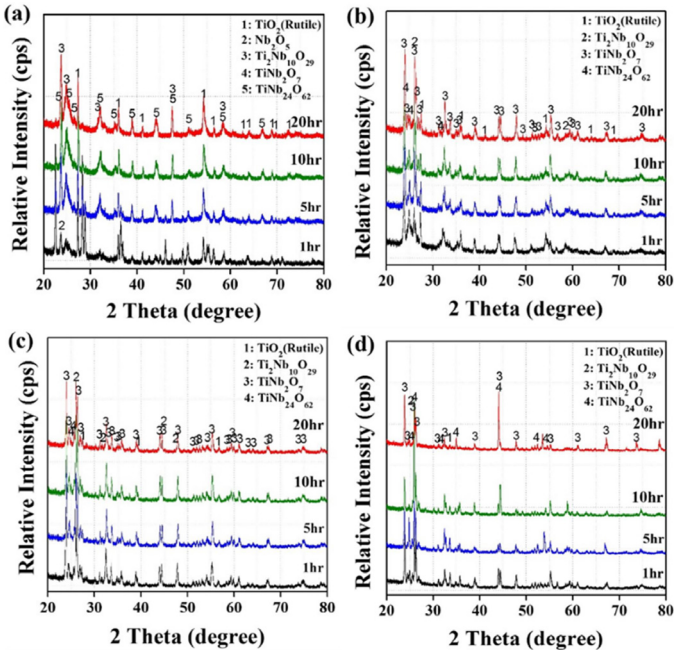

Fig. 5. XRD patterns of the Ti-Nb-O samples heat-treated at (a) 800°C, (b) 1000°C, (c) 1200°C, and (d) 1400°C

the predominant phase and is accompanied by small amounts of TiO_2, $TiNb_{24}O_{62}$, and $Ti_2Nb_{10}O_{29}$ phases. A similar trend can be seen for the sample heat-treated at 1200°C, as shown in Fig. 5c. As observed in this figure, the $TiNb_2O_7$ phase starts to appear as early as 1 h of processing time. However, for heat treatment at 1400°C, the $TiNb_{24}O_{62}$ content increases steadily with increase in the processing time, as shown in Fig. 5d.

Overall, the XRD results show that the Nb-rich phases tend to form first, according to the following stoichiometric complex oxide formation pathway: $TiNb_{24}O_{62} \rightarrow Ti_2Nb_{10}O_{29} \rightarrow TiNb_2O_7$. On the same token, some amount of rutile phase also exists in the a solid solution. The powder mixture begins to sinter with increase in processing time and temperature. In particular, at a processing temperature of 1400°C, there is considerable volume shrinkage with increase in the processing time, as shown in Fig. 6, which may be attributed to the sintering of the powder mixture due to the partial melting of the $TiNb_2O_7$ phase, whose melting point is very close to 1400°C (melting point of $TiNb_2O_7$ is 1450°C) [13]. The partial melting also explains the irregular increase in the $TiNb_{24}O_{62}$ content at 1400°C. The powder deviates from the stoichiometric oxide formation pathway because of the partial melting and re-solidification of the powder.

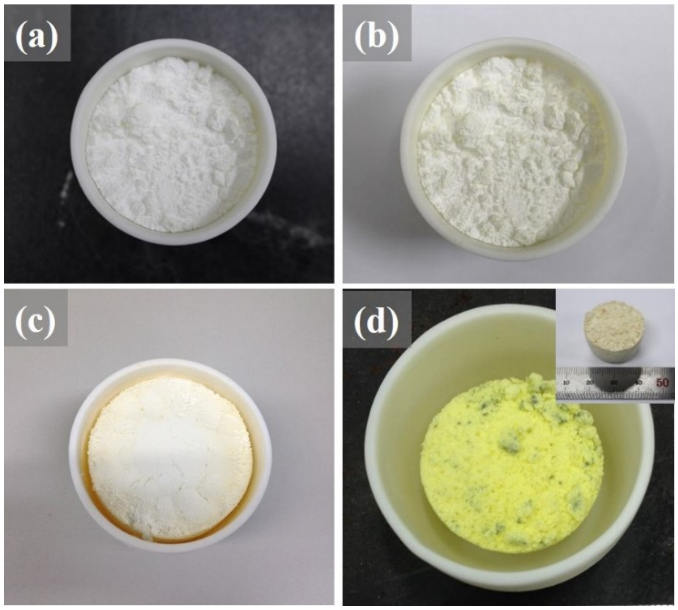

Fig. 6. Images of the Ti-Nb-O samples heat-treated at 1400°C for a) 1 h, b) 5 h, c) 10 h, and d) 20 h

Fig. 7 is a graphical representation of the QPA for $TiNb_2O_7$ by the Rietveld refinement method. Rietveld refinement is a method for fitting the entire XRD pattern and may be used to quantitatively determine crystallographic information of the specimen from the XRD results. Lattice parameters, lattice points, and space group information are required for fitting the measured XRD intensity peak profile satisfactorily. Results of the refinement analysis show that the overall proportion of the $TiNb_2O_7$ phase increases with increase in the processing time and temperature. At 800°C, there is no significant increase in the proportion of the $TiNb_2O_7$ phase with processing time. However, a dramatic increase in the $TiNb_2O_7$ content is observed with increase in the processing temperature. Further, at processing temperatures of 1000 and 1200°C, a similar trend is observation. The $TiNb_2O_7$ content increases rapidly with increase in the processing time from 1 to 5 h, beyond which the increase is gradual. An optimum phase ratio of more than 90 atomic % is obtained for a processing time of 20 h at 1200°C. Further, samples prepared at 1400°C show irregular phase content behavior owing to the partial melting and re-solidification of the powder, as explained earlier.

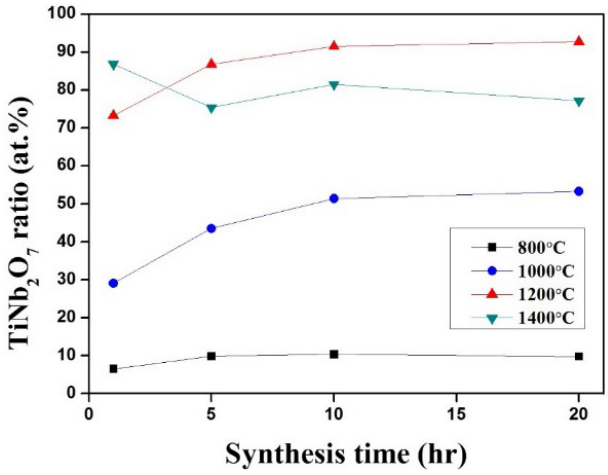

Fig. 7. Quantitative phase analysis of $TiNb_2O_7$ by the Rietveld refinement method

The morphologies of the as-synthesized Ti-Nb-O powders prepared at different synthesis times and temperatures are shown in Fig. 8. Generally, the synthesized powders have particles with relatively rough surfaces and irregular shapes, since the fine particles are found to form agglomerates during the synthesis process. The size and shape of the powders synthesized at 800°C are found to be similar to those of the initial TiO_2 and Nb_2O_5 powders. At 1000°C, the particles begin to sinter together owing to necking and the particle size increases significantly after 10 h

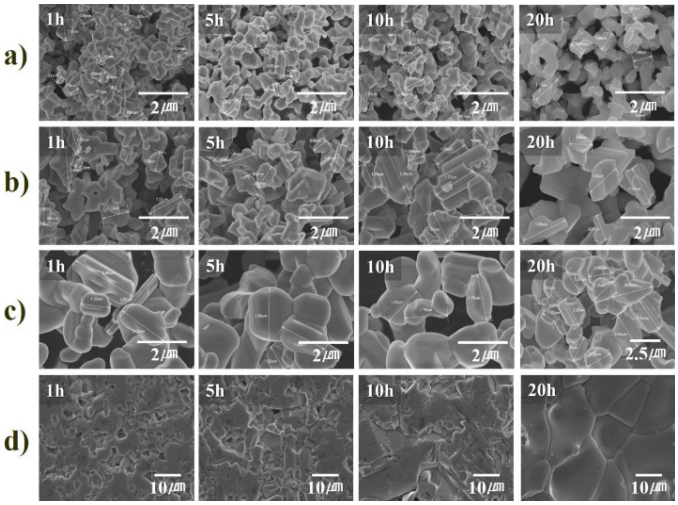

Fig. 8. Morphological evolution of the Ti-Nb-O samples heat-treated at a) 800°C, b) 1000°C, c) 1200°C, and d) 1400°C, over processing time

of processing. The necking process and size growth become even more significant for samples synthesized at 1200°C, whereas partial melting and sintering of the powder particles are observed at 1400°C, as shown in Fig. 8d.

Fig. 9 shows the particle size distribution of the Ti-Nb-O powders heat-treated at various temperatures (800-1200°C) for various reaction durations (1-20 h). All the powders show bi-modal particle size distribution. At 800°C, increase in the processing time has negligible effect on the particle size. The distribution curve shows irregular behavior owing to the low temperature and the low rate of reactant conversion, which results in particle agglomeration. On the other hand, at higher processing temperatures (1000 and 1200°C), the particle size gradually increases with increase in the processing time and the powder sample synthesized at 1200°C for 20 h shows a range of particle sizes from 1 to 10 µm. Three dimensional size distributions involving particle size metrics (d_{50}, d_{90}, and mean size), processing time, and temperature are also shown in Fig. 9d-f. The d_{50}, d_{90}, and mean size values after 20 h at 1200°C are 4.5,7.5, and 4.3 µm, respectively.

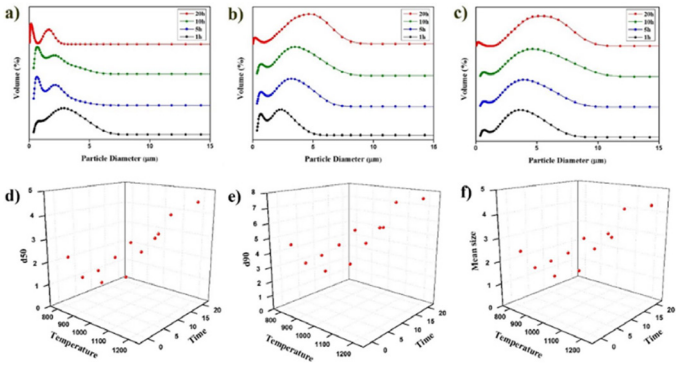

Fig. 9. Particle size analysis of the Ti-Nb-O powders heat-treated at a) 800°C, b) 1000°C, c) 1200°C. Values of d) d50, e) d_{90}, and f) mean size

3.3. Kinetics analysis of $TiNb_2O_7$

In order to understand the synthesis mechanism of $TiNb_2O_7$, kinetic analysis was performed. The reaction ratio (α) was defined as 0 before the reaction and 1 after completion of the reaction. The rate of each reaction was expressed as a function of the Arrhenius parameters according to the reaction model shown in (Eq. 1).

$$\frac{d\alpha}{dt} = k(T)f(\alpha) \tag{1}$$

where $\frac{d\alpha}{dt}$ is the reaction rate, α is the reaction ratio, $k(T)$ is a temperature dependent rate constant, t is the time, T is the temperature, and $f(\alpha)$ is the differential form of the reaction model [13].

In this study, the first-order reaction model $f(\alpha) = 1 - \alpha$ is used to describe the synthesis of the oxides. This model is applicable to a wide range of solid-state reactions that follow the general form Reactant (s) → Product (s) + Gas (g) [14].

The atomic percentage of the $TiNb_2O_7$ phase calculated by the Rietveld refinement method is presented in terms of the reaction ratio (α). Thus, a more general form of the first-order reaction equation can be written in the form of (Eq. 2).

$$-\ln(1-\alpha) = k(T)t \tag{2}$$

Therefore, by plotting $-\ln(1-\alpha)$ versus time (t), the rate constant (k) can be determined from the slope and intercept of the fitted straight line. Calculated values of the rate constants (k) are given in TABLE 2. The rate constant for the synthesis of $TiNb_2O_7$ for 20 h increases from 1.43×10^{-6} at 800°C and 1.06×10^{-5} at 1000°C to 3.64×10^{-5} at 1200°C. The dependence of the rate constant on the temperature is described by the Arrhenius law (Eq. 3).

TABLE 2

Rate constants k for the synthesized $TiNb_2O_7$ as a function of synthesis temperature and time

$TiNb_2O_7$	1 h	5 h	10 h	20 h
800 °C	1.86×10^{-5}	5.74×10^{-6}	3.03×10^{-6}	1.43×10^{-6}
1000 °C	9.52×10^{-5}	3.17×10^{-5}	2.00×10^{-5}	1.06×10^{-5}
1200 °C	3.66×10^{-4}	1.12×10^{-4}	6.85×10^{-5}	3.64×10^{-5}

$$k(T) = A\exp-\left(\frac{E_\alpha}{RT}\right) \tag{3}$$

In the above equation, A is a pre-exponential factor, $E\alpha$ is the activation energy, and R is the universal gas constant. The activation energies ($E\alpha$) calculated for synthesis temperatures in the range of 800-1200°C are 97.62 kJ/mol at 1 and 5h, 102.78 kJ/mol at10 h and 106.82 kJ/mol at 20 h, as shown in Fig. 10. This implies that at longer synthesis durations, more reactants are consumed, leading to a decrease in the reaction rate and consequently, an increase in the activation energy. In Table 3, the activation energies ($E\alpha$) and pre-exponential factor (A) values are shown as a function of synthesis duration.

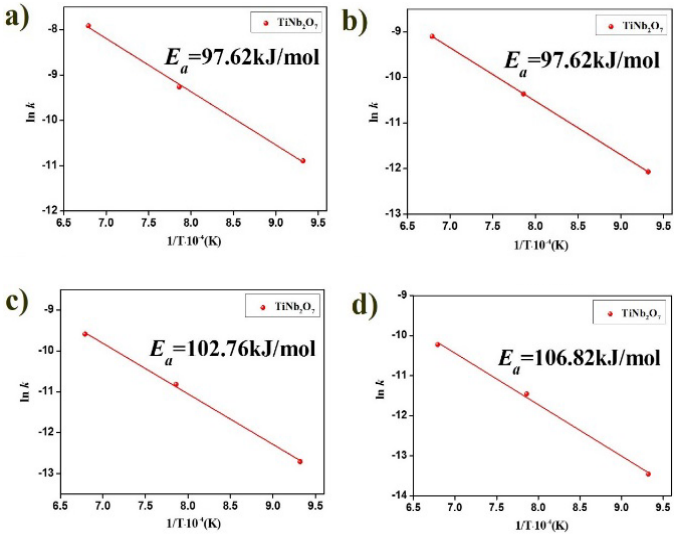

Fig. 10. Arrhenius plots for samples synthesized at temperatures in the range of 800-1200°C for a) 1 h, b) 5 h, c) 10 h, and d) 20 h

TABLE 3

Activation energy ($E\alpha$) and pre-exponential factor ($\ln A$) for various synthesis durations

$TiNb_2O_7$	$E\alpha$ (kJ/mol)	$\ln A$
1 h	97.62	0.03
5 h	97.62	–1.13
10 h	102.76	–1.16
20 h	106.82	–1.45

4. Conclusions

The possibility of synthesizing single-phase $TiNb_2O_7$ by solid-state reaction was examined in this study. A mixture of TiO_2 and Nb_2O_5 in a 1:1 molar ratio was heat-treated at various processing temperatures (800, 1000, 1200 and 1400°C) for various durations of time (1,5,10 and 20 h). It was found that Nb-rich phases tend to be formed first, following the stoichiometric complex oxide formation pathway $TiNb_{24}O_{62} \rightarrow Ti_2Nb_{10}O_{29} \rightarrow TiNb_2O_7$. The optimum processing time and temperature for $TiNb_2O_7$ synthesis were found to be 20 h and 1200°C, respectively, and under these conditions, the maximum $TiNb_2O_7$ phase content of over 90 atomic % was obtained with an average particle size of about 4.3 µm. Complete conversion of raw materials into $TiNb_2O_7$ was not possible because some amount of rutile phase always existed as a solid solution with $TiNb_2O_7$. Overall, the proportion of the $TiNb_2O_7$ phase increased with increase in the processing time and temperature. Beyond a processing temperature of 1400°C, partial melting and re-solidification of the mixture occurred resulting in the formation of a hard bulk compact instead of a powder. The rate constant and activation energy were calculated from the QPA data. The activation energies ($E\alpha$) calculated for synthesis temperatures in the range of 800-1200°C were 97.62 kJ/mol for 1h and 5h, 102.78 kJ/mol at10h and 106.82 kJ/mol at 20 h.

Acknowledgments

This research was supported by an internal R&D program of the Korea Institute of Industrial Technology (KITECH), funded by the Ministry of Strategy and Finance, Korea and partially supported by the technology innovation program, 10063427, Development of eco-friendly smelting technology for the production of rare metal production for lowering manufacturing costs using solid oxide membrane funded by the Ministry of Trade, Industry & Energy

REFERENCES

[1] C. Jo, Y. Kim, J. Hwang, J. Shim, K. Chun, J. lee, Chem Mater. **26**, 3508 (2014).
[2] B. Guo, X. Yu, XG. Sun, M. Chi, ZA. Qiao, J. Liu, YS. Hu, XQ. Yang, JB. Goodenough, S. Dai, Energy Environ Sci. **7**, 2220 (2014).
[3] C.M. Reich, A. Kaiser, JTS. Irvine, Fuel Cells. **1**, 249 (2001).
[4] E. Da Costa, C.O. Avellaneda, A. Pawlicka, J. Mat. Sci. **36**, 1407 (2001).
[5] B.C. Yadav, A.K. Srivastava, P.K. Khanna, Int. J. Green. Nanotechnol. **3**, 160 (2011).
[6] R.A. Jat, P. Samui, N.K. Gupta, P.S.C. Parida, Thermochim. Acta. **592**, 31 (2014).
[7] L.E. Depero, L. Sangaletti, B. Allieri, M. Notaro, J. Mat. Res. **13**, 1644 (1998).
[8] M. Hirano, Y. Ichihashi, J. Mater. Sci. **44**, 6135 (2009).
[9] R.S. Roth, L.W. Coughanour, J. Res. Nat. Bur. Stand. **55**, 209 (1955).
[10] A.D. Wadsley, Acta Crystallogr. **14**, 660 (1961).
[11] A.D. Wadsley, Acta Crystallogr. **14**, 664 (1961).
[12] R.S. Roth, A.D. Wadsley, Acta Crystallogr. **18**, 724 (1965).
[13] K.U. Santosh, Chemical kinetics and reaction dynamics. New Delhi: Springer, 2006.
[14] E.H. James, Principles of chemical kinetics. 2nd ed. New York: Academic Press, 2007.